INFLUENCE OF THICKNESS ON THE VALUES OF STRESS INTENSITY FACTOR IN COMPACT TENSION SPECIMEN

Germana FERNANDÉZ[1,3], Petr MIARKA[2,3], Stanislav SEITL[2,3]

[1]Department of Construction and Manufacturing Engineering, University of Oviedo, Campus de Viesques, Módulo 1 - Planta Baja s/n 33203, Gijón, Spain
[2]Institute of Physics of materials, Czech Academy of Sciences, Žižkova 513/22 616 00, Brno, Czech Republic
[3]Institute of Structural Mechanics, Faculty of Civil Engineering Brno University of Technology; Veveří 331/95, 602 00 Brno, Czech Republic

UO243770@uniovi.es, miarka@ipm.cz, seitl@ipm.cz

DOI: 10.35181/tces-2021-0014

Abstract. *It is well known that value of fracture toughness depends on the thickness of studied specimen. This paper deals with an assessment of the influence of the thickness on the values of stress intensity factor measured at crack tip in the compact-tension specimen. For this a numerical model was assembled representing different specimen's thicknesses and material characteristics. From this 3D numerical model, the SIF values were calculated using by direct extrapolation method.*

Keywords

CT specimen, SIF, Thickness, Fracture.

1. Introduction

The compact tension (CT) specimen, see Fig. 1, is commonly used in the experimental measurements of the fatigue crack growth rates in metallic materials evaluated by Paris' law [1].

Furthermore, the standard for such measurements ASTM E647 [2] recommends the minimum thickness to achieve plane strain conditions and to have constant crack increment over the load cycles. The recommendation has following form:

$$\frac{W}{20} \leq B \leq \frac{W}{4}, \quad (1)$$

where the B is the specimen thickness and W is the characteristic dimension of CT specimen. Nonetheless the influence of the specimen's thickness has not been investigated in detail.

The influence of the free surface on the fatigue crack growth as well as the specimen thickness was numerically analyzed in [4] and recently it was both studied numerically and experimentally on two different materials by Oplt et. al in [5]. These studies broaden the understanding of crack front curvature formation on the specimens with constant thickness. However, the crack front curvature might vary as the stress conditions in the middle of the specimen are considered to be plane strain, while on the surface, it is considered to be plane stress.

For example, traditional size of CT specimen with $W = 50$ mm, the stress conditions for very thin specimen with a thickness $B < 2.5$ mm are believed to be as plane stress while for the specimens with thickness $B > 10$ mm it is acting as plane strain. However, the practical material testing sometimes require to prepare specimens with different thicknesses.

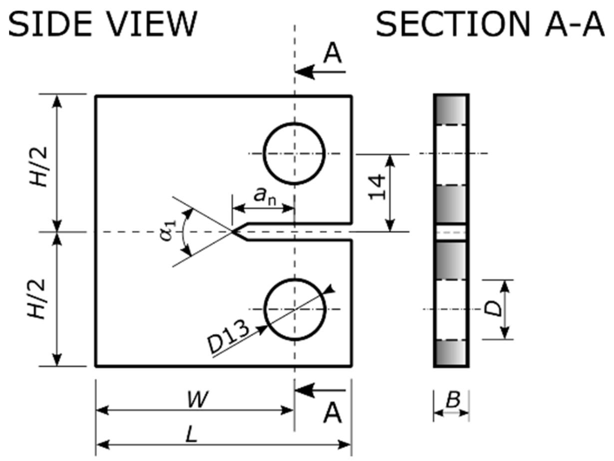

Fig. 1: Compact tension specimen

Furthermore, recent study showed influence of the constraint effect on the fatigue crack growth rate [3] evaluated by digital image correlation (DIC) method. Nonetheless, there was no comparison of different specimen thickness and more importantly no direct comparison between numerically generated and experimentally measured displacement fields. The intent of this numerical study, is to create 3D numerical model and to analyze influence of various thicknesses on the values of stress intensity factor (SIF). This numerical model and its generated numerical results will serve to design and analyze the DIC experimental analysis.

2. Theoretical Background

This numerical study is based on linear elastic fracture mechanics (LEFM) concept. The LEFM uses the Williams expansion (WE) [6] for the description of the stress fields in a close vicinity of the crack tip of homogeneous isotropic cracked material. The WE can be expressed for mode I as:

$$\sigma_{i,j} = \frac{K_I}{\sqrt{2\pi r}} f_{i,j}^{I}(\theta) + O_{i,j}(\theta) \quad (2)$$

where $\sigma_{i,j}$ represents stress tensor, K_I is the stress intensity factor (SIF) for mode I, r, θ are the polar coordinates (provided in the centre of the coordinate system at the crack tip; crack faces lie along the x-axis), $f_{i,j}^{I}(\theta)$ are known shape functions, $O_{i,j}$ represent higher order terms.

A CT specimen was used due to its simple shape, relatively simple experimental set up and due to well described stress fields using up to five WE coefficients, which provides extensive use of CT specimen in measurement of fatigue parameters for various materials. During a fatigue test, a SIF range K_I is used, which is calculated by using Eq. 3 according to standard ASTM E647 6 [2].

$$K_I = \frac{P}{B\sqrt{W}} \frac{(2+\alpha)}{(1-\alpha)^{\frac{3}{2}}} (0.886 + 4.64\alpha - 13.32\alpha^2 + 14.72\alpha^3 - 5.6\alpha^4), \quad (3)$$

where α is the relative crack length expressed as a/W, a is the crack length, W is the width of the specimen, B is the thickness of the specimen and P is the applied load range. The literature offers various books with database of the geometry functions used in the SIF calculation i.e. [7] and in [8].

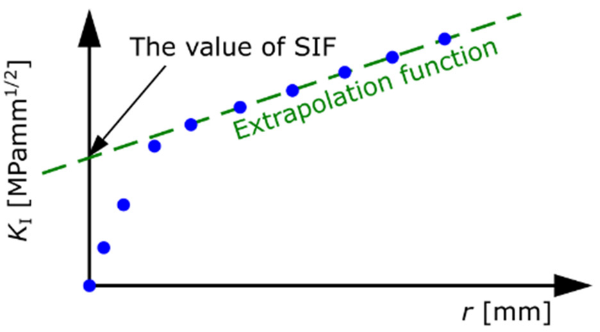

Fig. 2: Direct extrapolation method used in evaluation of SIF.

In the numerical study, the SIF was calculated using the direct extrapolation method. This method is based on the generated stress distribution in a cracked specimen and extrapolates the value of SIF at the location of crack tip i.e. $r = 0$. The calculation can be expressed as:

$$K_I = \lim_{r\to 0}(\sigma \cdot \sqrt{2\pi r}), \quad (4)$$

where σ is the crack opening stress. Furthermore the extrapolation process is shown in following figure:

3. Numerical Model

In order to analyse the above-mentioned problems a three-dimensional (3D) numerical model in commercial finite element (FE) method software ANSYS [9] was created. The numerical model of the CT specimen had the dimensions mentioned in Fig. 1:(a) and material is considered to be linear elastic. Linear elastic material model was chosen based on the assumption of the use of LEFM.

The studied geometry of CT specimen had dimension of length L of 62.5 mm, height H of 60 mm and width W of 50 mm, the specimen's thickness B varied from 1 ÷ 20 mm. The analyzed relative crack lengths α were 0.3; 0.5; 0.8 and 0.9.

The input material parameters were Young's Modulus E = 210 GPa and Poisson's ratio ν varied from 0 ÷ 0.49. The numerical model was meshed with tetrahedral quadratic 20-node elements (SOLID186) (see Fig. 3:). In total 24 180 elements with 106 260 nodes were used in FE model. The Basic element size length ahead of crack was 0.075 mm with increasing size towards the model's edges. Further from the crack tip region, the coarser mesh with size of 2 mm was adopted and 12 elements along the thickness were used.

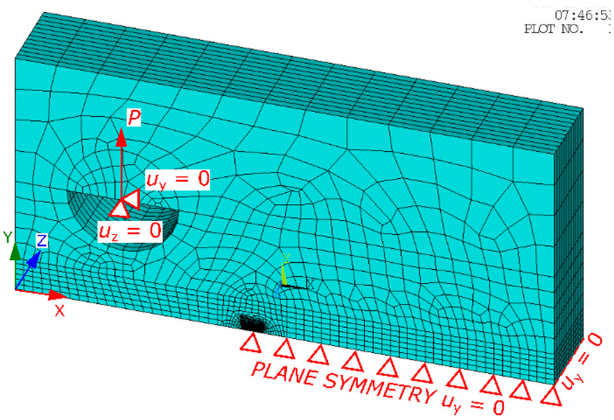

Fig. 3: Numerical model and boundary conditions.

The specimen was then constrained to create symmetry conditions (u_y = 0). Adequate boundary conditions were added to prevent rigid body translation (See Fig. 3).

The structured mesh around the crack was adopted to reduce numerical error, while keeping the calculation in real time. The crack tip refinements and its structured mesh are presented following figure.

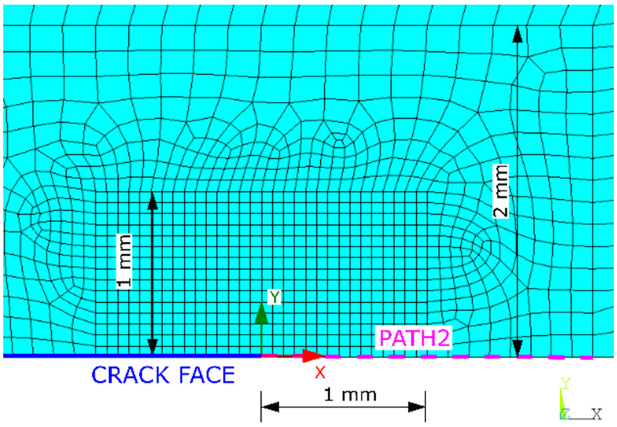

Fig. 4: Crack tip detail with path for results extractions.

Since the given geometry of CT specimen allows to use an advantage of existing symmetry, only half of the specimen was modelled. The model was loaded with the force *P* at the pin hole. The values of *P* were calculated based on Eq. 2 and the value itself varied based on the crack length α and specimen's thickness *B* to achieve constant value of K_I = 10 MPam$^{1/2}$ see Fig. 5:. Please note that the force *P* is decreasing due to reduced specimen's stiffness due to increased crack length *a*.

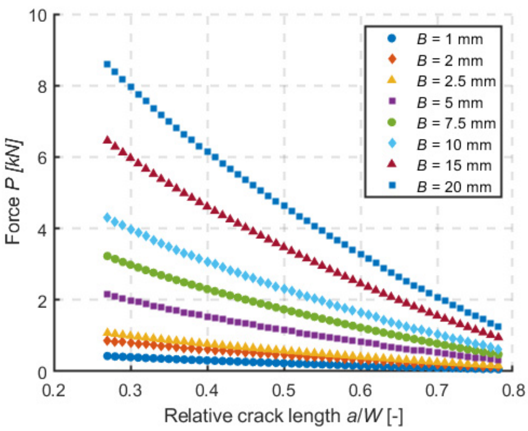

Fig. 5: Equivalent force to produce constant value of K_I = 10 MPam$^{1/2}$ based on different thickness.

Furthermore, two paths for extrapolation of the SIF values were used, i.e. first one on the specimen's surface (*B* = 0) while the other one was located in the middle of the thickness (*B*/2). Both paths are shown in following figure.

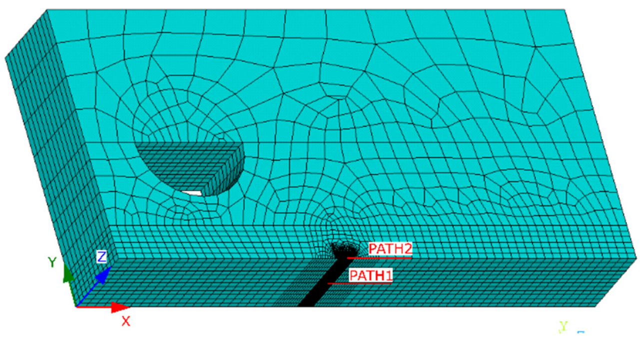

Fig. 6: Paths used for numerical results extrapolation.

4. Numerical results

To examine 3D numerical model, a parametric numerical study was performed with varying Poisson's ratio from 0 ÷ 0.49 and such numerical results of σ_{yy} were used in the calculation of K_I values from both paths by direct method. The calculated values of K_I for various crack lengths of α = 0.3; 0.5 and 0.8 evaluated from both PATH1 (middle of the specimen) and PATH2 (specimen's surface).

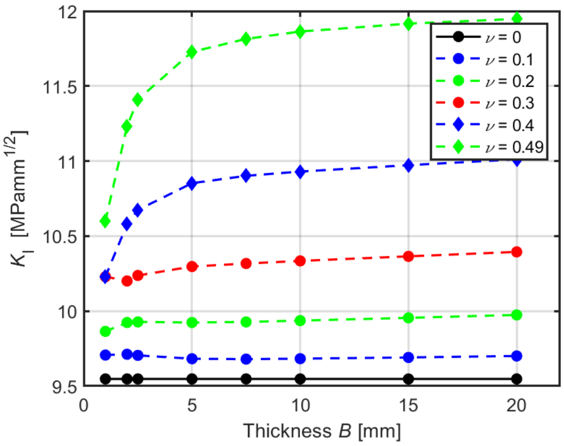

Fig. 7: Calculated values of K_I for α = 0.3 and PATH1 (middle).

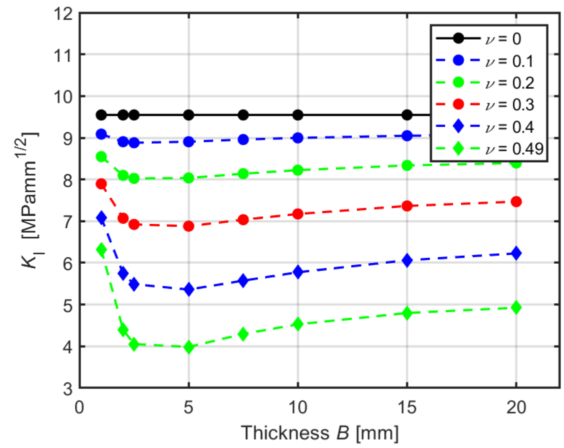

Fig. 8: Calculated values of K_I for α = 0.3 and PATH2 (surface).

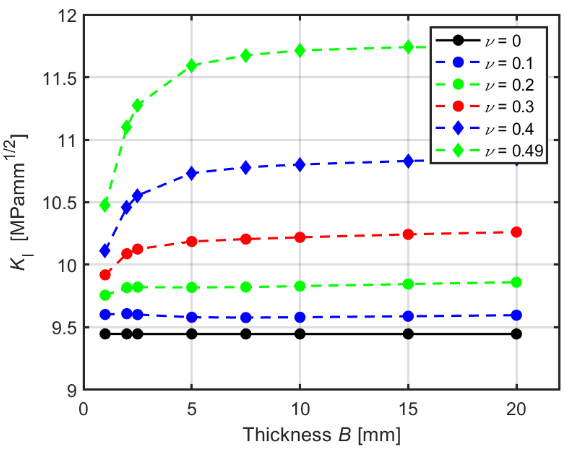

Fig. 9: Calculated values of K_I for α = 0.5 and PATH1 (middle).

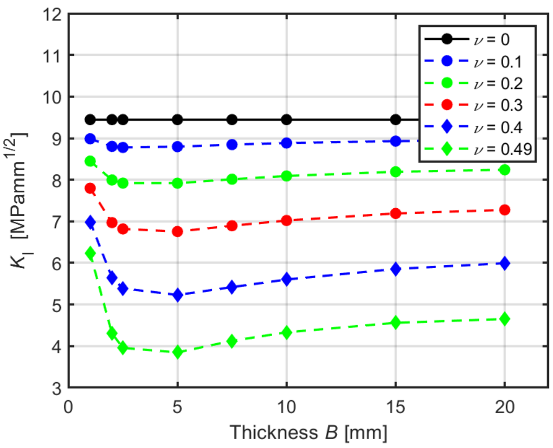

Fig. 10: Calculated values of K_I for $\alpha = 0.5$ and PATH2 (surface).

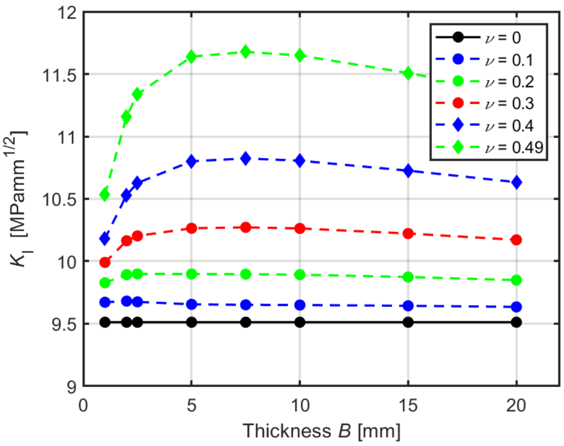

Fig. 11: Calculated values of K_I for $\alpha = 0.8$ and PATH2 (middle).

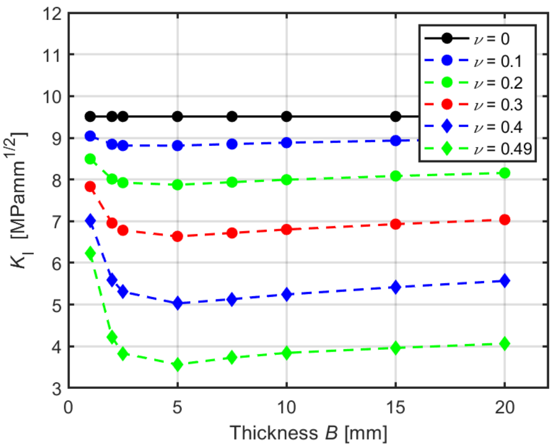

Fig. 12: Calculated values of K_I for $\alpha = 0.8$ and PATH2 (surface).

The above presented numerical results show influence of the Poison's ratio on the values of K_I and as well the influence of the specimen's thickness B. The numerical results with $\nu = 0$ shows constant value of K_I throughout the studied cases, while the Poisson's ratio $\nu = 0.49$ shows highest difference in obtained values. Moreover, the difference in the values of K_I is clear observable for results obtained on the surface of the specimen, where the values differ by nearly 55 % for $B = 2.5$ mm and $\nu = 0.49$.

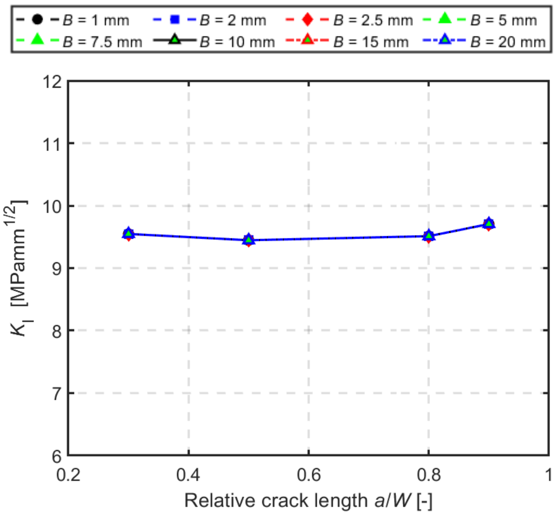

Fig. 13: Variation of K_I values based on the different crack length for $\nu = 0$ and for PATH1 (middle).

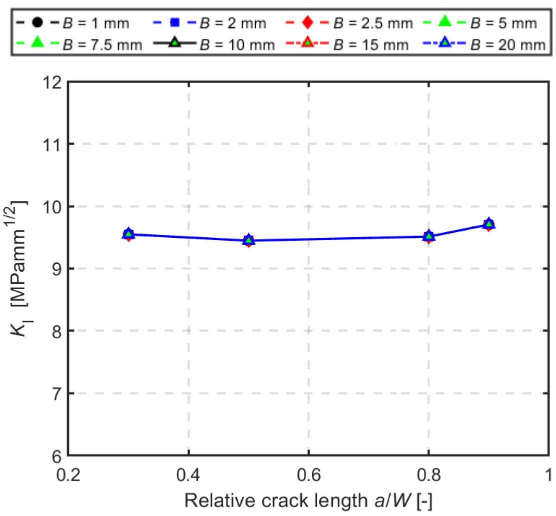

Fig. 14: Variation of K_I values based on the different crack length for $\nu = 0$ and for PATH2 (surface).

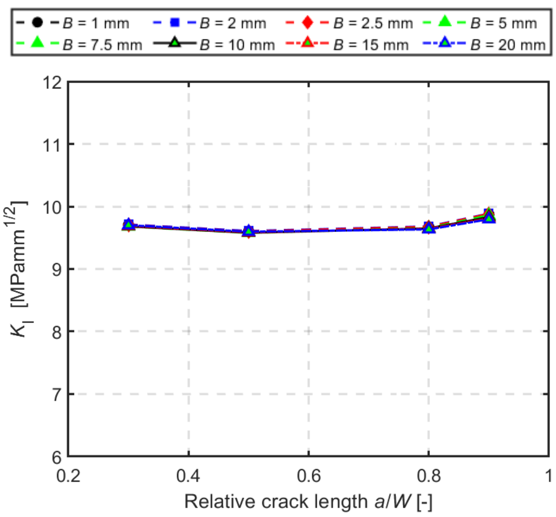

Fig. 15: Variation of K_I values based on the different crack length for $\nu = 0.2$ and for PATH1 (middle).

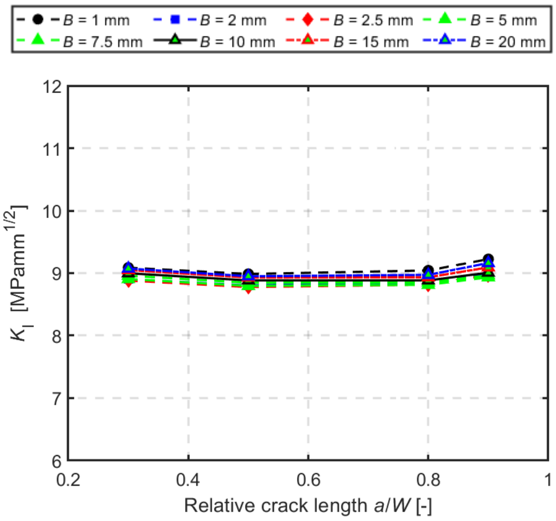

Fig. 16: Variation of K_I values based on the different crack length for $\nu = 0.2$ and for PATH2 (surface).

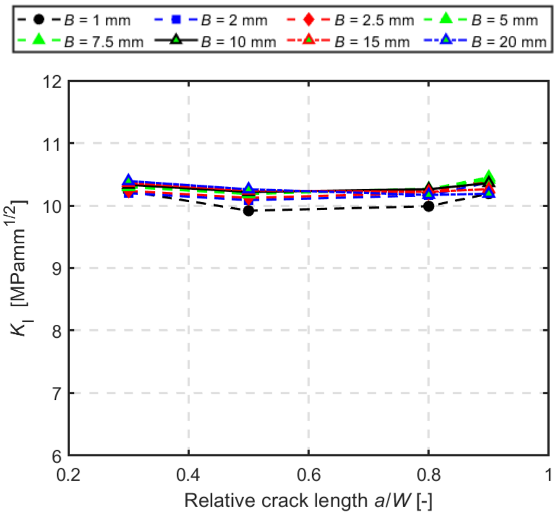

Fig. 17: Variation of K_I values based on the different crack length for $\nu = 0.3$ and for PATH1 (middle).

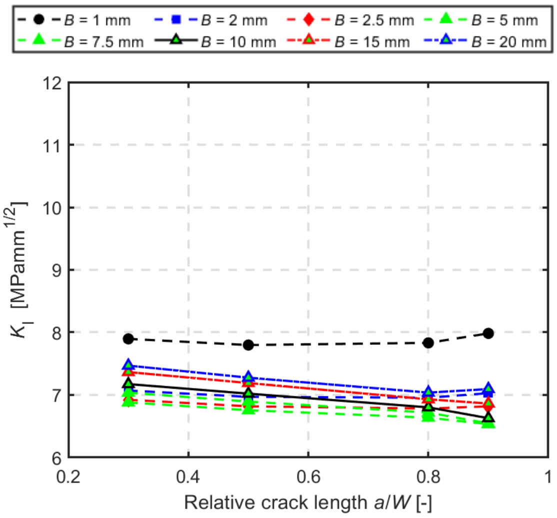

Fig. 18: Variation of K_I values based on the different crack length for $\nu = 0.3$ and for PATH2 (surface).

All of these obtained results for different crack lengths and thicknesses as presented in Fig. 13 to Fig. 18 again confirm the observation in Fig. 7 to 12 as the difference in K_I values increases with the increasing value of Poisson's ratio as well as with the increasing specimen's thickness B. The results obtain from surface differ with higher error from the ones obtained from the middle of the specimen. Furthermore, the variations for the K_I values for different specimen's thickness is also related to fact that the original standard was proposed for specimens with thickness B = 10 mm, while in practice the thickness may vary.

This fact should be considered when the DIC experimental measurement is prepared as it is gathering the displacements fields from the surface of the specimen. This can greatly influence the accuracy in obtained values of the evaluated fracture an fatigue properties.

5. Conclusions

The influence of thickness on the SIF value as obtain on the geometry of compact tension specimen has been investigated. The following conclusion can be drawn:

The presented study showed influence of the specimen's thickness on the values of SIF.

In addition to this, the numerical results showed influence of the Poisson's ratio on these values. Based on these finding, the numerical model with curved crack front has to be model to generate same value of K_I on the surface to have same as in the middle of the specimen. Such numerical results can be directly compared with the DIC experimentally obtained displacements fields.

Acknowledgements

The financial support of the grants No. FAST-J-21-7340 and from Czech Science Foundation with project no. 20-00761S is greatly appreciated.

References

[1] PARIS, P. and F. ERDOGAN. A Critical Analysis of Crack Propagation Laws, *Journal of Basic Engineering*, 1963, iss. 85, pp. 528-533. ISSN 0098-2202. DOI: 10.1115/1.3656900

[2] ASTM E647-15e1, Standard Test Method for Measurement of Fatigue Crack Growth Rates. In: ASTM International, West Conshohocken, PA; 2015

[3] MIARKA, P., A.S. CRUCES, S. SEITL, L. MALÍKOVÁ and P. LOPE□-CRESPO. Influence of the constraint effect on the fatigue crack growth rate in S355 J2 steel using digital image correlation. *Fatigue Fracture of Engineering Materials*

Structures. 2020, vol. 43, iss. 8, pp. 1703–1718. DOI: 10.1111/ffe.13198

[4] ŠEVČÍK, M., P. HUTAŘ, M. □OUHAR, and L. NÁHLÍK. Numerical estimation of the fatigue crack front shape for a specimen with finite thickness. *International Journal of Fatigue*. 2012, vol. 39, pp. 75-80. ISSN: 0142-1123. DOI: 10.1016/j.ijfatigue.2011.03.010

[5] OPLT, T., P. HUTAŘ, P. POKORNÝ, L. NÁHLÍK, □. CHLUP and F. BERTO. Effect of the free surface on the fatigue crack front curvature at high stress asymmetry. *International Journal of Fatigue*. 2019, vol. 118, pp. 249–261. ISSN: 0142-1123. DOI: 10.1016/j.ijfatigue.2018.08.026

[6] WILLIAMS ML. On the Stress Distribution at the Base of a Stationary Crack. *Journal of Applied Mechanics.* 1956;24(1):6.

[7] TADA H, PARIS PC, and G.R, IRWIN, American Society of Mechanical Engineers., ASM International. *The stress analysis of cracks handbook.* 3rd ed. New York: ASME Press: Professional Engineering Pub. : ASM International; 2000.

[8] CARPINTERI A. *Handbook of Fatigue Crack Propagation in Metallic Structures.* Elsevier Science; 1994.

[9] ANSYS® Academic Research Mechanical, Release 19.2, 2018.

About Authors

Germana FERNANDEZ was born in Gijón, she received her MSC. degree after successful defence her master thesis in June 2021 at FCE BUT.

Petr MIARKA was born in Český Těšín, Czech Republic received his Ph.D. in 2021 at the Institute of Structural Mechanics, FCE BUT via defence of his doctoral thesis entitled: Analysis of mixed mode I/II failure of selected structural concrete grades. His research interests include evaluation of fatigue and fracture parameters, preparation of specimens for fatigue tests and work with experimental output, numerical simulations, and fracture resistance analysis.

Stanislav SEITL was born in Přerov, Czech Republic. He is an associate professor at FCE BUT and a leader of FRACTIGUE group at IPM CAS. His research interests consist in fatigue of civil engineering materials and lifetime estimation, two-parameter fracture mechanics, numerical modelling and calculations of fracture-mechanics parameters.